J|A|C|S

A R T I C L E S

Biocatalytic Synthesis of a Nanostructured and Crystalline Bimetallic Perovskite-like Barium Oxofluorotitanate at Low Temperature

Richard L. Brutchey, Edward S. Yoo, and Daniel E. Morse*

Contribution from the Institute for Collaborative Biotechnologies, California NanoSystems Institute, the Materials Research Laboratory, and the Department of Molecular, Cellular and Developmental Biology, University of California, Santa Barbara, California 93106

Received May 4, 2006; E-mail: d_morse@lifesci.ucsb.edu

Abstract: Silicatein, an enzymatic biocatalyst from the marine sponge *Tethya aurantia*, is demonstrated to catalyze and template the hydrolysis/condensation of the molecular precursor $BaTiF_6$ at low temperature to form nanocrystalline $BaTiOF_4$, an orthorhombic oxofluorotitanate. The kinetics of hydrolysis and growth were studied in-situ via pH profiling and quartz crystal microbalance (QCM) techniques. The composition and structure of the resulting $BaTiOF_4$ microstructures on the silicatein surface were characterized using FT-IR spectroscopy, X-ray photoelectron spectroscopy, energy-dispersive X-ray spectroscopy, scanning electron microscopy, transmission electron microscopy, and selected area electron diffraction. The silicatein-mediated hydrolysis/condensation of $BaTiF_6$ generates nanocrystalline $BaTiOF_4$ (a high-temperature intermediate to $BaTiO_3$) at 16 °C without any added acid or base, and the growth is templated along the protein filaments into floret microstructures. The unique combination of silicatein and the single-source molecular precursor has allowed a multimetallic perovskite-like material to be biocatalytically synthesized, in vitro, for the first time.

I. Introduction

Nature possesses an extraordinary and unique ability to assemble inorganic ions into a wide range of complex micro- and nanoarchitectures (e.g., endo- and exoskeletal frameworks,[1,2] crystalline magnetite in magnetotactic bacteria,[3] optic lenses of trilobites,[4] gravity sensing otolith crystals,[5] etc.). An astonishing characteristic of many biominerals is that they are produced in nonequilibrium systems that delicately organize the movements of ions into a (oftentimes crystalline) structure while operating at ambient pressure, temperature, and pH values close to neutral.[6] One example is the ability of biological systems to control the exquisite nanostructures of hydrated amorphous silica (e.g., the skeletons of diatoms, radiolarians, and sponges) with a precision and detail that exceeds human engineering capabilities.[7]

Investigation of the mechanism governing the biological synthesis of silica structures in a marine sponge (*Tethya aurantia*) led to the surprising discovery that this synthesis is mediated, in part, by a family of structure-directing enzymes, named silicateins (for **silica** pro**teins**), occluded within the silica

structural elements of the marine sponge.[8] Silicateins were found to simultaneously catalyze and structurally direct (i.e., template) the hydrolysis and condensation of tetraethyl orthosilicate in vitro to form silica.[9] The silicateins exhibit catalytic activity at neutral pH and low temperature (for a reaction that typically requires the extremes of pH or temperature) and a templating activity that directs the anisotropic growth of silica particles along the axial protein filament. Silicatein filaments also demonstrated the ability to form gallium oxide and titanium dioxide from molecular precursors in vitro—two inorganic semiconductors that biological species have never naturally produced.[10,11] The crystalline nanoparticles of gallium oxide formed by this process demonstrate a preferential alignment directed by the underlying protein filament, revealing a pseudo-epitaxial, structure-directing activity of the biomolecular template. In addition, the proteins function at low temperatures (16–25 °C), yet generate and stabilize high-temperature crystal polymorphs of gallium oxide (γ-phase) and titanium dioxide (anatase), thus providing further evidence of their template-directed, structure-controlling activity. Although remarkable in its scope, thus far only simple unimetallic oxide materials have been biocatalytically generated and templated by silicatein.

(1) Aizenberg, J.; Weaver, J. C.; Thanawala, M. S.; Sundar, V. C.; Morse, D. E.; Fratzl, P. *Science* **2005**, *309*, 275.
(2) Aizenberg, J.; Muller, D. A.; Grazul, J. L.; Hamann, D. R. *Science* **2003**, *299*, 1205.
(3) Sakaguchi, T.; Burgess, J. G.; Matsunaga, T. *Nature* **1993**, *365*, 47.
(4) Towe, K. M. *Science* **1973**, *179*, 1007.
(5) Sollner, C.; Burghammer, M.; Busch-Nentwich, E.; Berger, I.; Schwarz, H.; Riekel, C.; Nicolson, T. *Science* **2003**, *302*, 282.
(6) Mann, S. *Chem. Commun.* **2004**, 1.
(7) Perry, C. C.; Keeling-Tucker, T. *J. Biol. Inorg. Chem.* **2000**, *5*, 537.

(8) Shimizu, K.; Cha, J.; Stucky, G. D.; Morse, D. E. *Proc. Natl. Acad. Sci. U.S.A.* **1998**, *95*, 6234.
(9) Cha, J. N.; Shimizu, K.; Zhou, Y.; Christiansen, S. C.; Chmelka, B. F.; Stucky, G. D.; Morse, D. E. *Proc. Natl. Acad. Sci. U.S.A.* **1999**, *96*, 361.
(10) Kisailus, D.; Choi, J. H.; Weaver, J. C.; Yang, W.; Morse, D. E. *Adv. Mater.* **2005**, *17*, 314.
(11) Sumerel, J. L.; Yang, W.; Kisailus, D.; Weaver, J. C.; Choi, J. H.; Morse, D. E. *Chem. Mater.* **2003**, *15*, 4804.

Applying biocatalytic structure-directing routes to multi-metallic perovskite and perovskite-like materials is of interest because they represent a technologically important class of materials that possesses a wide range of useful electronic, magnetic, and optical properties.[12] For example, multimetallic perovskites are used as ferroelectrics,[13] piezoelectric transducers,[14] solid oxide fuel cells,[15] high-temperature superconductors,[16] thermoelectrics,[17] ferromagnets,[18] capacitors,[19] IR detectors,[20] and colossal magnetoresistors.[21] Traditional methods for the preparation of multimetallic perovskite and perovskite-like materials are hampered by the requirements for a precisely controlled stoichiometry of the metals, the need for highly mixable metal precursors, closely matched reaction rates of the metal precursors, and harsh conditions (e.g., extreme temperature, pressure, or pH) favorable for formation of a particular crystal phase. Oftentimes, segregation into two or more crystalline or amorphous phases occurs as a result of these complicating factors.[22,23] Single-source molecular precursors provide a route to circumvent many of these challenges. A preexisting and intimate geometric relationship between two or more metals in one discrete molecular complex (e.g., M^1-E-M^2 bond linkages or strong ion pairings) has been proven to produce a higher abundance of M^1-E-M^2 bond linkages upon conversion to the target material under conventional high-temperature synthesis methods.[24] Through a combination of biocatalytic structure-directing synthesis and single-source molecular precursors, the possibility arises to access complex materials via low-temperature routes in which the biomolecular template can influence particle size and crystallization.

Barium fluorotitanate ($BaTiF_6$) has been previously identified as a potential single-source molecular precursor to barium titanate ($BaTiO_3$).[25] The complex contains barium and titanium in the requisite 1:1 stoichiometry, and the solid-state structure consists of intimately associated cubooctahedrally coordinated barium and octahedrally coordinated titanium atoms, coordination geometries matching those present in the perovskite structure of $BaTiO_3$.[26] Here we report, for the first time, that an enzymatic biocatalyst can template a nanostructured bimetallic perovskite-like material in vitro. The silicatein filaments are capable of catalytic hydrolysis/condensation of $BaTiF_6$ at low temperature to yield an unusual and crystalline barium oxofluorotitanate, $BaTiOF_4$, where the perovskite-like material is anisotropically templated along the silicatein filaments in floret microstructures composed of nanostructured petals.

II. Experimental Details

Chemicals and General Procedures. Water was filtered through a Milli-Q purification system to yield a resistivity ≥ 18 MΩ cm^{-1}. Tris·HCl (tris(hydroxymethyl)aminomethane hydrochloride, 99+%), hexafluorotitanic acid (99.9%), and barium nitrate (99.999%) were purchased from Aldrich and used without further purification. The barium fluorotitanate ($BaTiF_6$) precursor was prepared according to literature procedure and isolated as a white microcrystalline solid.[25] The identity of the microcrystalline solid was confirmed by powder X-ray diffraction (XRD). In addition, single crystals were grown by evaporation of an aqueous solution of the complex over several weeks (25 °C), and single crystal X-ray analysis confirmed that the unit cell parameters matched those previously reported for the structure of $BaTiF_6$.[26]

Silicatein filaments were isolated and purified according to a method previously described.[9] Thermal denaturation was accomplished by heating a dispersion of the filaments in 25 mM Tris·HCl buffer (90 °C) for 60−90 min. The filaments (native and thermally denatured) were isolated by centrifugation and used immediately thereafter.

Silicatein-Catalyzed Synthesis of BaTiOF₄. A 0.013 M aqueous solution of $BaTiF_6$ (1.0 mL) and a 0.39 M aqueous solution of H_3BO_3 (0.1 mL) were simultaneously added to a 1.6-mL polyethylene centrifuge tube containing silicatein filaments (ca. 1.25 mg). The solution was vigorously agitated and the sample was placed on a rotary stirrer (16 °C for 24 h). The product was isolated by centrifugation at 13 000 rpm for 10 min. Residual precursor in the supernatant was decanted away from the solid product, and the product was then rinsed with water followed by centrifugation (3 × 1.0 mL), dried at 25 °C for 24−48 h, and stored in a desiccator. Parallel experiments were performed with native and denatured filaments.

Pyrolysis of BaTiF₆ Precursor. Pyrolysis experiments (25 mg $BaTiF_6$) were performed from 27 to 850 °C on an Anton Parr HTK 16 high-temperature platinum heating stage controlled via thermocouple at a rate of 10 °C min^{-1} in air, and the conversion was monitored by in-situ XRD.

Characterization. pH measurements were performed on a Accumet Research AR60 pH meter. To measure the pH of the reaction, the reaction was increased by 4× scale to achieve enough volume for accurate measurements. Quartz crystal microbalance (QCM) measurements were performed on a Q-Sense D300 instrument using the axial flow chamber and a quartz crystal sensor with a 100 nm gold coating (Q-Sense QSX 301, AT-cut, 5 MHz). The filaments were adsorbed onto the quartz crystal in-situ (as observed by a drop in frequency) by flowing a dispersion of the filaments over the Au surface until a stable frequency baseline was established, and then the precursor solution was introduced. The resonant frequency was measured at intervals of 40 ms (20 °C for 19 h). Changes in mass were qualitatively calculated using the Sauerbrey equation for quartz ($\Delta m = -17.7$ ng Hz^{-1} cm^{-2}·$\Delta f/n$, where m is the adsorbed mass, f is the frequency, and n is the overtone number) and the induction period was calculated according to $i = t_c - m_c/r_c$ (where t_c is the reaction time at which the growth rate was constant, m_c is the deposited mass at t_c, and r_c is the growth rate at t_c).[27] XRD analyses were performed on a Bruker D8 Advance X-ray diffractometer with an Anton Parr HTK 16 high-temperature stage using Cu Kα radiation. Scanning electron microscopy (SEM) was performed on a Tescan Vega 5130 microscope at an operating voltage of 20 kV. Energy-dispersive X-ray spectroscopy (EDX, IXRF Systems) was performed in conjunction with SEM to qualitatively determine the elemental composition of the samples. EDX calibration was performed against an internal standard, and the data were demonstrated to be accurate. Transmission electron microscopy (TEM) analyses were

(12) Bhalla, A. S.; Guo, R.; Roy, R. *Mater. Res. Innovat.* **2000**, *4*, 3.
(13) Rüdiger, A.; Schneller, T.; Roelofs, A.; Tiedke, S.; Schmitz, T.; Waser, R. *Appl. Phys. A* **2005**, *80*, 1247.
(14) Nagarajan, V.; Roytburd, A.; Stanishevsky, A.; Prasertchoung, S.; Zhao, T.; Chen, L.; Melngailis, J.; Auciello, O.; Ramesh, R. *Nature Mater.* **2003**, *2*, 43.
(15) Huang, K. Q.; Feng, M.; Goodenough, J. B.; Milliken, C. *J. Electrochem. Soc.* **1997**, *144*, 3620.
(16) Bednorz, J. G.; Muller, K. A. *Z. Phys. B: Condens. Matter* **1986**, *64*, 189.
(17) Terasaki, I.; Sasago, Y.; Uchinokura, K. *Phys. Rev. B: Condens. Matter Mater. Phys.* **1997**, *56*, 12685.
(18) Jonker, G. H.; Vansanten, J. H. *Physica* **1950**, *16*, 337.
(19) Basceri, C.; Streiffer, S. K.; Kingon, A. I.; Waser, R. *J. Appl. Phys.* **1997**, *82*, 2497.
(20) Ludlow, J. H.; Mitchell, W. H.; Putley, E. H.; Shaw, N. *J. Sci. Instrum.* **1967**, *44*, 694.
(21) Ramirez, A. P. *J. Phys.: Condens. Matter* **1997**, *9*, 8171.
(22) Hubert-Pfalzgraf, L. G. *J. Mater. Chem.* **2004**, *14*, 3113.
(23) Gao, Y.; Koumoto, K. *Cryst. Growth Des.* **2005**, *5*, 1983.
(24) Fujdala, K. L.; Brutchey, R. L.; Tilley, T. D. Tailored Oxide Materials Via Thermolytic Molecular Precursor (TMP) Methods. In *Topics in Organometallic Chemistry*; Copéret, C., Chaudret, B., Eds.; Springer-Verlag: New York, 2005; vol. 16, pp 69−116.
(25) Lee, M. K.; Tung, K. W.; Cheng, C. C.; Liao, H. C.; Shih, C. M. *J. Phys. Chem. B* **2002**, *106*, 4963.
(26) Becker, S.; Benner, G.; Hoppe, R. *Z. Anorg. Allg. Chem.* **1990**, *591*, 7.
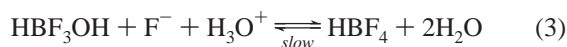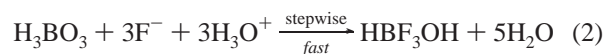(27) Deki, S.; Aoi, Y.; Asaoka, Y.; Kajinami, A.; Mizuhata, M. *J. Mater. Chem.* **1997**, *7*, 733.

carried out on a FEI Tecnai G^2 Sphera microscope at an operating voltage of 200 kV. Selected area electron diffraction (SAED) patterns were collected from 20 randomly selected regions at a camera distance of 100 cm. Samples for TEM studies were prepared by depositing hexanes suspensions of the samples onto carbon-coated copper grids obtained from Ted Pella, Inc. X-ray photoelectron spectroscopy (XPS) was performed on a Kratos Axis Ultra XPS system using a monochromated aluminum anode. The binding energy of C 1s in all spectra was standardized to 285 eV. FT-IR spectra were obtained on a Nicolet Magna 850 IR spectrometer, and samples were prepared as KBr pellets. Thermogravimetric analysis (TGA) was performed on a Mettler TGA/sDTA851e at a heating rate of 10 °C min^{-1} under flowing air/nitrogen.

III. Results and Discussion

Synthesis Conditions and Hydrolysis/Growth Kinetics. The hydrolytic stability of the BaTiF$_6$ precursor complex in water makes it uniquely tractable for use in aqueous systems. The Partial Charge Model (PCM) predicts that the degree of hydrolysis (*h*) for BaTiF$_6$ in the pH range of 2−3 is less than 0.45 (eq 1, see Supporting Information).[28]

$$BaTiF_6 + 2hH_2O \rightleftharpoons BaTiF_{6-h}(OH)_h + hF^- + hH_3O^+ \quad (1)$$
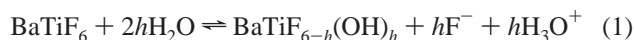
Indeed, Schmitt, Grove, and Brown reported that the degree of hydrolysis for BaTiF$_6$ in water ranged from 0.06 to 0.12 for concentrations of BaTiF$_6$ between 0.02 and 0.01 M, respectively.[29] To verify this result, the pH of a 0.013 M solution of BaTiF$_6$ was monitored over time. According to the reaction equilibrium established in eq 1, a reduction in pH will occur as the molecular precursor hydrolyzes; we observed that over the course of 8 days, no observable change in pH occurred, as anticipated. Addition of a Lewis acid to scavenge free F$^-$ ions effectively shifts the equilibrium toward hydrolysis. Boric acid, H$_3$BO$_3$, reacts rapidly with 3 molar equivalents of F$^-$ ions in a stepwise manner to yield HBF$_3$OH, which slowly reacts with a fourth equivalent of F$^-$ to yield HBF$_4$ (eqs 2, 3).[30]

$$H_3BO_3 + 3F^- + 3H_3O^+ \xrightarrow[fast]{stepwise} HBF_3OH + 5H_2O \quad (2)$$

$$HBF_3OH + F^- + H_3O^+ \underset{slow}{\rightleftharpoons} HBF_4 + 2H_2O \quad (3)$$

Accumulation of the weak acids (HBF$_3$OH and HBF$_4$) will also lower the pH of the solution as the reaction proceeds over time.

To test the possibility that silicatein can biocatalytically promote the low-temperature hydrolysis and condensation of BaTiF$_6$, an aqueous solution of BaTiF$_6$ (0.013 mmol) and H$_3$BO$_3$ (0.039 mmol) were added to freshly isolated silicatein filaments at 16 °C and the reaction mixture was allowed to incubate for 24 h. Indeed, under these conditions, the silicatein filaments did catalytically hydrolyze BaTiF$_6$ in the presence of H$_3$BO$_3$ as a fluoride scavenger, as observed by a reduction in pH of the aqueous solution in the presence of native silicatein at 16 °C (Figure 1). After a 180 min induction period, the pH of the reaction mixture gradually decreased from a value of 3.03, with the maximum rate of reduction in pH occurring shortly thereafter, and a final pH of 2.76 being reached after 1440 min as a result of the accumulation of the weakly acidic hydrolysis byproducts. The induction period is potentially a result of
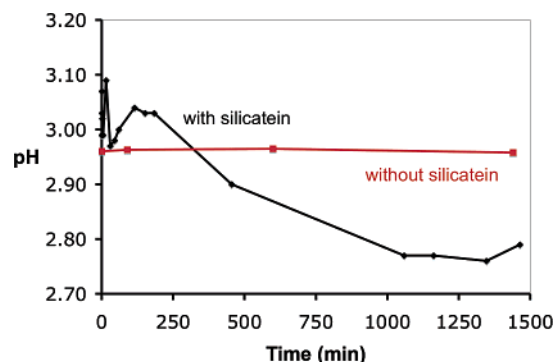
(28) Henry, M.; Jolivet, J. P.; Livage, J. *Struct. Bonding* **1992**, *77*, 153.
(29) Schmitt, R. H.; Grove, E. L.; Brown, R. D. *J. Am. Chem. Soc.* **1960**, *82*, 5292.
(30) Wamser, C. A. *J. Am. Chem. Soc.* **1948**, *70*, 1209.

Figure 1. Representative hydrolysis kinetics measured by monitoring the pH of aqueous BaTiF$_6$ (0.052 mmol)/H$_3$BO$_3$ (0.16 mmol) as a function of time with and without the silicatein biocatalyst (ca. 5 mg) at 16 °C.

H$_3$BO$_3$ preferentially scavenging free fluoride from the autohydrolysis of BaTiF$_6$ (eq 1) before reacting with fluoride released from the silicatein-catalyzed hydrolysis.[27] Preincubating the aqueous solution of BaTiF$_6$ and H$_3$BO$_3$ for 75 min prior to introduction of the silicatein filaments resulted in a 60% reduction in the induction period, which supports the hypothesis of H$_3$BO$_3$ scavenging the solution of any free fluoride before biocatalytic hydrolysis occurs. The biocatalytic activity of the silicatein is supported by the observed stability of BaTiF$_6$ in the presence of H$_3$BO$_3$ under identical reaction conditions. Addition of 2 molar equivalents of H$_3$BO$_3$ per F$^-$ ion of BaTiF$_6$, with no silicatein, yielded a solution that was stable for 24 h at 16 °C (i.e., the solution maintained optical clarity and the pH remained constant over the experimental time course).

A quartz crystal microbalance (QCM) is a highly sensitive surface mass detector (sensitivity in the nanogram range) that measures mass as a function of the change in frequency of a piezoelectric quartz crystal when it is perturbed by the adhesion of small objects.[31] QCM analyses can be carried out in a liquid environment, making it particularly useful in this context to measure in-situ growth kinetics on the proteins in an aqueous environment. Silicatein filaments were adhered to the gold surface of a QCM sensor crystal in-situ by flowing a dispersion of the filaments over the crystal followed by introduction of the precursor solution. For the in-situ growth study, 80 μL total volume of BaTiF$_6$ (0.94 μmol) and H$_3$BO$_3$ (2.8 μmol) was introduced to the silicatein filaments on the surface of the sensor crystal and the mass change (Δm) as a result of product growth was monitored continuously over the reaction time (Figure 2). After an induction period of 50 min, the growth rate increased until a maximum rate was reached at 210 min. This maximum growth rate was maintained for approximately 130 min, and then the rate slowly decreased over the remainder of the reaction time, potentially as a result of enzyme deactivation, depletion of the molecular precursor, or a combination of both. The growth kinetics, as measured by QCM analysis, closely mirrors the hydrolysis kinetics taken under similar conditions − suggesting that hydrolysis and nucleation/growth proceed simultaneously during the course of the reaction. Furthermore, a solution of BaTiF$_6$ (0.94 μmol) and H$_3$BO$_3$ (2.8 μmol), in the absence of silicatein, demonstrated no change in mass over time as measured by QCM, which is concordant with not observing a reduction in pH for the same solution (vide supra).

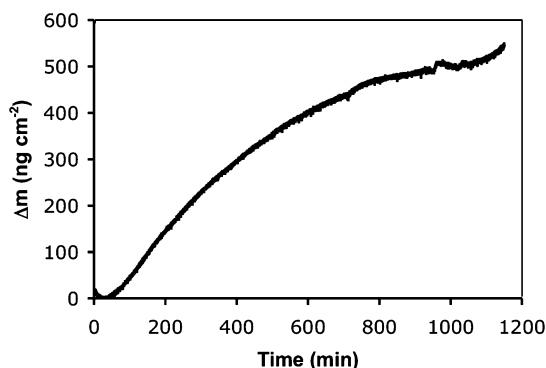(31) Bruckenstein, S.; Shay, M. *Electrochim. Acta* **1985**, *30*, 1295.

Figure 2. Qualitative relationship between BaTiOF$_4$ growth on silicatein filaments (Δm) and reaction time at 20 °C (0.94 μmol BaTiF$_6$ and 2.8 μmol H$_3$BO$_3$ precursor solution).

Composition and Structure. The composition of the resulting material was characterized by FT-IR spectroscopy, X-ray photoelectron spectroscopy (XPS), and energy-dispersive X-ray spectroscopy (EDX). The FT-IR spectrum of the BaTiF$_6$ molecular precursor displays a strong band at 569 cm^{-1} that has been previously assigned to an asymmetric stretching mode ν_3(TiF$_6^{2-}$).[32,33] The FT-IR spectrum of the reaction product grown on the silicatein filaments displays three strong bands at 1655, 1529, and 592 cm^{-1} in addition to weak bands at 854 and 492 cm^{-1} (see Supporting Information). The strong bands at 1655 and 1529 cm^{-1} are assigned to vibrations of the amide functionalities in the protein filaments. The remaining bands are not present in a control spectrum of native silicatein filaments and originate from the inorganic product. The bands at 592 and 492 cm^{-1} are a combination of Ti–F stretching modes, and the weak band at 854 cm^{-1} is assigned to vibrations of Ti–O–Ti oxygen bridges.[34-36] Additionally, a strong asymmetric stretching band ν_3(CO$_3^{2-}$) at 1425 cm^{-1} is absent, indicating the inorganic product is free of carbonate (a common impurity in barium containing perovskites).[37] On the basis of FT-IR analysis, the inorganic product thus appeared to contain both Ti–O and Ti–F bonds in the structure.

XPS was used to corroborate the FT-IR data and quantify the surface elemental composition of the material (Figure 3). The Ba 3d$_{5/2}$ and F 1s binding energies measured for the reaction product grown on the silicatein filaments were 780.0 and 684.5 eV, respectively. For comparison, the Ba 3d$_{5/2}$ binding energies observed for BaTiO$_3$ and BaTiF$_6$ are 779 and 780 eV, respectively.[38] The binding energy for Ti 2p$_{3/2}$ was observed as a broad orbital at 459.5 eV. Further analysis of the Ti 2p$_{3/2}$ orbital revealed that ca. 81% of the Ti^{4+} was at a higher binding energy (459.5 eV), whereas the balance was at a slightly lower binding energy (458.5 eV), which may suggest the presence of two slightly different surface environments. The Ti^{4+} binding energy should be more sensitive to the coordination environment since the titanium is closely associated with the octahedrally
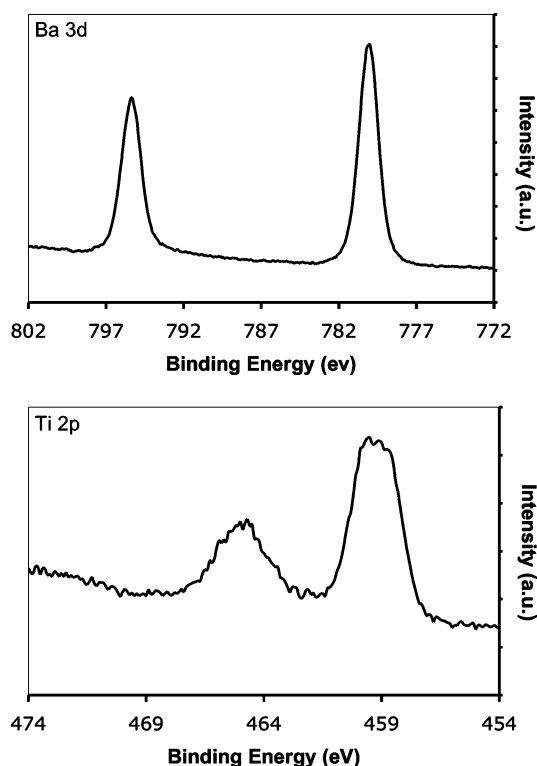
(32) Peacock, R. D.; Sharp, D. W. A. *J. Chem. Soc.* **1959**, 2762.
(33) Dean, P. A. W.; Evans, D. F. *J. Chem. Soc. A* **1967**, 698.
(34) Laptash, N. M.; Maslennikova, I. G.; Kaidalova, T. A. *J. Fluorine Chem.* **1999**, *99*, 133.
(35) Ingat'eva, L. N.; Polishchuk, S. A.; Antokhina, T. F.; Buznik, V. M. *Glass Phys. Chem.* **2004**, *30*, 139.
(36) Sengupta, A. K.; Adhikari, S. K.; Dasgupta, H. S. *J. Inorg. Nucl. Chem.* **1979**, *41*, 161.
(37) López, M. D. B.; Fourlaris, G.; Rand, B.; Riley, F. L. *J. Am. Ceram. Soc.* **1999**, *82*, 1777.
(38) Tsunekawa, S.; Ito, S.; Mori, T.; Ishikawa, K.; Li, Z.-Q.; Kawazoe, Y. *Phys. Rev. B: Condens. Matter Mater. Phys.* **2000**, *62*, 3065.

Figure 3. High-resolution Ba 3d and Ti 2p XPS spectra of BaTiOF$_4$/silicatein filament composite.
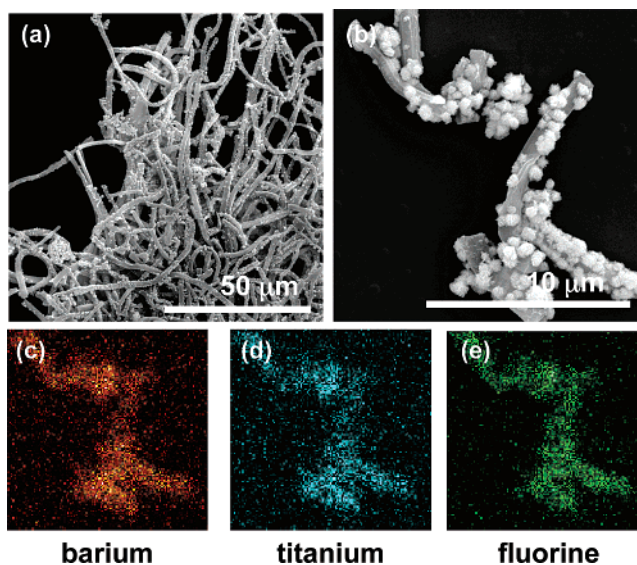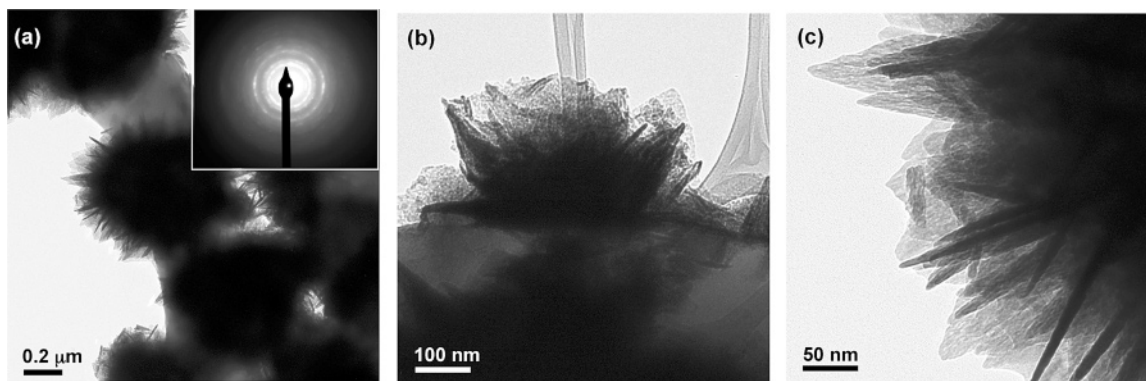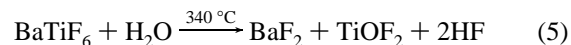

Figure 4. (a, b) BaTiOF$_4$ florets catalytically grown and templated by native silicatein filaments at 16 °C. EDX elemental maps (of image shown in b) for (c) barium, (d) titanium, and (e) fluorine.

coordinated anions. The binding energy observed for Ti^{4+} in the reaction product is intermediate between those observed for the octahedral metal oxide and the metal fluoride (i.e., the Ti 2p$_{3/2}$ binding energies observed for BaTiO$_3$ and BaTiF$_6$ are 458 and 462 eV, respectively).[38] This is in agreement with the FT-IR data suggesting a mixed barium oxofluorotitanate, BaTiO$_n$F$_{6-n}$, structure for the reaction product. Indeed, a stoichiometric amount of fluoride and barium are present in the surface composition of the material relative to titanium. The surface composition of F/Ti was determined, on average, to be 2.1:1.

Figure 5. (a−c) TEM micrographs of BaTiOF$_4$ florets on the surface of silicatein filaments formed from the hydrolysis/polycondensation of BaTiF$_6$. (Inset) Representative SAED pattern of nanocrystalline BaTiOF$_4$.

In addition, the surface composition of Ba/Ti was on average 0.7:1. The elemental composition of the reaction product was also qualitatively mapped using EDX in conjunction with scanning electron microscopy (SEM). It is evident from the elemental maps (Figure 4b−e) that fluorine is intimately associated with the barium and titanium present in the reaction product on the surface of the silicatein filaments. Moreover, barium, titanium, and fluorine were not detected by EDX on the surface of the heat-denatured silicatein filaments.

Thermogravimetric analysis of the inorganic/silicatein filament composites demonstrated a precipitous weight loss from successive dehydration and combustion of the proteinaceous material between 100 and 700 °C (see Supporting Information). On average, the inorganic/silicatein filament composites were ca. 36 wt % proteins based on TGA. As a result of the low BaTiF$_6$ precursor concentration and/or the small crystallite size of the product, a sufficient amount of sample was not obtained for analysis by powder X-ray diffraction (XRD). Analysis of the inorganic/silicatein composites by transmission electron microscopy (TEM) and selected area electron diffraction (SAED) did, however, reveal the presence of nanocrystalline material with calculated *d*-spacings (±0.02 Å) of 3.48, 2.92, and 2.20 Å (Figure 5), which correspond to 3 of the most intense reflections for orthorhombic BaTiOF$_4$, a perovskite-like bimetallic oxofluorotitanate.[36] The structure is composed of infinite chains of corner sharing *cis*-TiO$_2$F$_4$ octahedra, linked via oxygen atoms, with the (TiO$_2$F$_4$)$_n^{2n-}$ chains coupled to one another via *n* cubooctahedrally coordinated Ba^{2+} atoms.[39] The BaTiOF$_4$ is formed as a dispersed coating of floret microstructures (mean diameter 708 ± 39 nm) adhered to the surface of the silicatein filaments (Figure 4). Without H$_3$BO$_3$ the biocatalytic synthesis of BaTiOF$_4$ did not proceed (as verified by SEM and XPS), while addition of greater than a 2× molar excess of H$_3$BO$_3$ per equivalent of fluoride in BaTiF$_6$ did not change the structure or morphology of the product. Also, when heat-denatured silicatein filaments were used, no reaction product on the surface of the filaments was observed, suggesting that the structure-directing activity of the filaments was dependent upon the 3-dimensional structure of the constituent proteins. The hydroxyl groups displayed on the native silicatein surface, which have been previously implicated in having a role in bio-templating,[8,10]

may influence the nucleation and/or growth of BaTiOF$_4$ on the filament surface.[40]

Investigation into the solid-state pyrolysis of BaTiF$_6$ provides insight into the chemical and structural transformations of BaTiF$_6$ in the presence of silicatein (Figure 6). The precursor complex is stable in air until elevated temperatures (ca. 340 °C), demonstrating that BaTiF$_6$ is thermally stable in addition to being hydrolytically stable. Thermal conversion of BaTiF$_6$ occurred over two well-defined weight-loss events as established by TGA.[41] The first weight-loss event occurred over the range of 340−550 °C, and the end ceramic yield corresponded to the loss of 2 equiv of F$^-$ via hydrolysis and condensation (eq 4 or 5).

$$BaTiF_6 + H_2O \xrightarrow{340\,°C} BaTiOF_4 + 2HF \qquad (4)$$

$$BaTiF_6 + H_2O \xrightarrow{340\,°C} BaF_2 + TiOF_2 + 2HF \qquad (5)$$

Crystalline BaTiOF$_4$ (orthorhombic) and BaF$_2$ (Frankdicksonite) were observed by XRD after pyrolysis to 500 °C, a result of the partial hydrolysis/condensation and structural rearrangement of BaTiF$_6$ with atmospheric water at high temperature. The second weight loss occurred over the range of 550−1000 °C, and the final ceramic yield corresponded to complete conversion to BaTiO$_3$ via loss of 4 additional equivalents of F$^-$ (eq 6).

$$BaTiOF_4 + 2H_2O \xrightarrow{550\,°C} BaTiO_3 + 4HF \qquad (6)$$
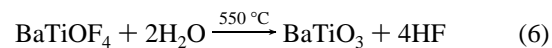
Heating to 850 °C induces another phase transition to crystalline BaTiO$_3$ (cubic), following total hydrolysis and condensation of BaTiOF$_4$. Remarkably, biocatalytic hydrolysis and condensation of BaTiF$_6$ in the presence of silicatein allows for the nucleation and growth of nanocrystalline BaTiOF$_4$ (a high-temperature mixed oxofluorotitanate intermediate to BaTiO$_3$) at 16 °C and 1 atm without any added acid or base. Moreover, the silicatein-catalyzed conversion yields phase-pure BaTiOF$_4$—without the presence of an additional segregated BaF$_2$ crystalline phase that is typically observed in the high-temperature pyrolysis of BaTiF$_6$. In contrast to these results, the few previously reported synthetic protocols for the unique oxofluorotitanate have required either high pressure and temperature (1283 atm, 350 °C)[39] or an acid-promoted hydrolysis/condensation from mixed titanium and barium salts.[38]

(39) Crosnier, M. P.; Fourquet, J. L. *Eur. J. Solid State Inorg. Chem.* **1992**, *29*, 199.

(40) Bäuerlein, E. *Angew. Chem., Intl. Ed.* **2003**, *42*, 614.

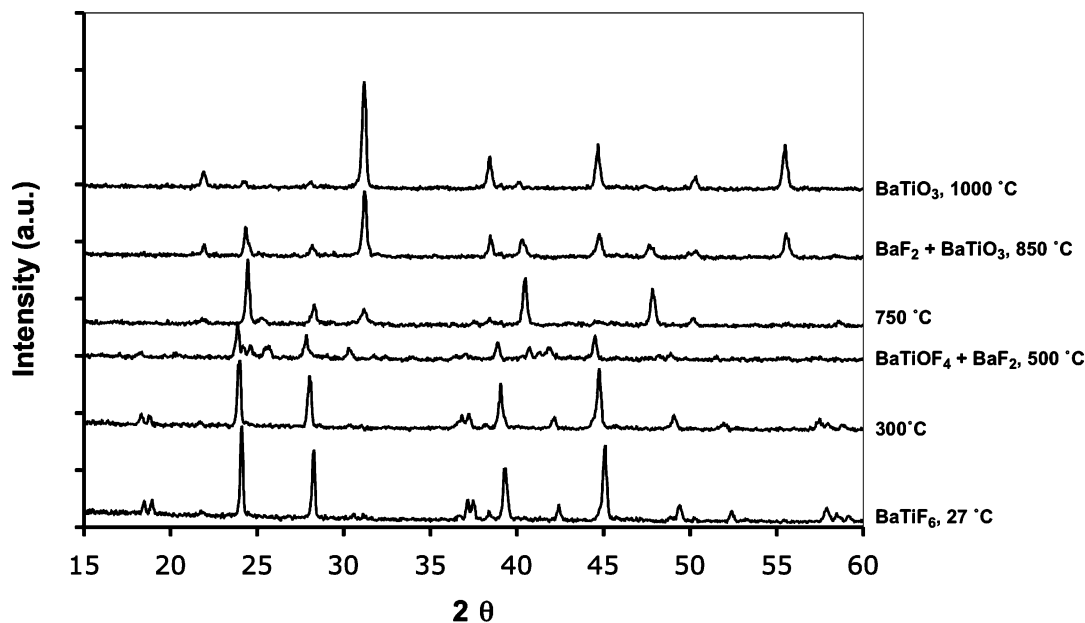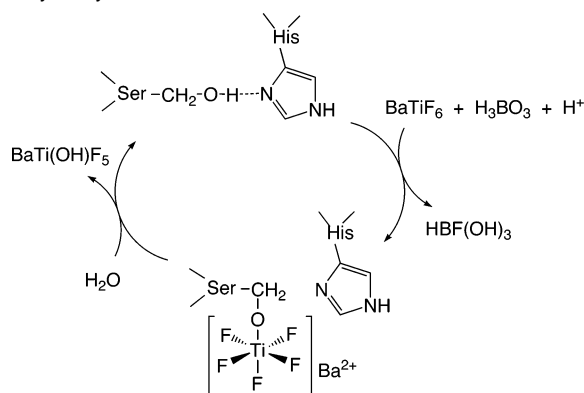(41) Heilbron, M. A.; Gellings, P. J. *Thermochim. Acta* **1976**, *17*, 97.

Figure 6. Temperature-dependent phase transformations from the pyrolysis of $BaTiF_6$.

Scheme 1. Proposed Mechanism of Catalysis of $BaTiF_6$ Hydrolysis by Silicatein

Proposed Mechanism. Previous analyses of the protein and DNA sequence databases revealed the surprising result that silicatein is a member of the cathepsin L family of proteolytic (protein hydrolyzing) enzymes, with the hydroxyl of serine and an imidazole nitrogen of histidine side chains H-bonded at the catalytic active site.[8] Site-directed mutagenesis confirmed the hypothesis that the H-bonding interaction between the serine and histidine increases the nucleophilicity of the serine side chain, facilitating attack of the oxygen on the substrate metal center.[42] Silicatein-mediated catalytic hydrolysis previously has proven viable for metalloid alkoxides,[9] metal alkoxide hydroxides,[11] and metal hydrates.[10] Here, it is proposed that the increased nucleophilicity of the serine side chain facilitates the initial hydrolysis of $BaTiF_6$ metal fluoride in the presence of H_3BO_3 (Scheme 1). The $BaTi(OH)F_5$ complex would then undergo an additional catalyst-mediated hydrolysis step with an equivalent of water to yield $BaTi(OH)_2F_4$.

Complexation by anions such as F^- can have a profound influence on the hydrolysis/condensation of metal species. The PCM predicts that for a given metal complex, complexation with anionic species will occur if the electronegativity of the resulting metal complex is higher than the electronegativity of the anion and lower than the electronegativity of the protonated anionic species (i.e., $\chi_{F^-} \leq \chi_{Ti(IV)} \leq \chi_{HF}$).[28] On the basis of a comparison of electronegativites in this system, the PCM predicts that both complexes, $BaTi(OH)F_5$ and $BaTi(OH)_2F_4$, are indeed accessible. Calculated electronegativity−pH curves for fluoride complexation to 6-coordinate Ti^{4+} confirm that complexation can occur over a wide pH range from $-5.6 <$ pH < 8.4, also supporting the possibility of fluoride complexation under the working conditions of this system (pH 2−3).[43] Once $BaTiF_6$ is converted to $BaTi(OH)_2F_4$ via silicatein-mediated hydrolysis, condensation through an oxolation mechanism would yield $BaTiOF_4$ (eq 7).[28]

$$BaTi(OH)_2F_4 \xrightarrow{\text{oxolation}} BaTiOF_4 + H_2O \qquad (7)$$

IV. Conclusions

A multimetallic perovskite-like material has, for the first time, been biocatalytically synthesized and templated. A low-temperature silicatein-mediated hydrolysis/condensation of $BaTiF_6$ was successfully utilized for the slow growth of nanocrystalline $BaTiOF_4$ along the protein filaments at 16 °C. In-situ monitoring of the pH and mass gain revealed that the maximum rates of hydrolysis and growth occur after ca. 200 min. In the absence of silicatein, the $BaTiF_6$ precursor solution was stable under identical conditions, whereas in the absence of H_3BO_3, silicatein did not produce the crystalline $BaTiOF_4$ product−demonstrating the necessity of both silicatein and H_3BO_3 for growth of the oxofluorotitanate. The $BaTiOF_4$ grows as floret microstructures composed of nanostructured petals along the silicatein filaments. The hydroxyl groups displayed on the silicatein surface may play a role in nucleation and/or growth of the nanocrystalline $BaTiOF_4$ on the native protein filaments. Heat denaturation of the silicatein, which disrupts the 3-dimensional protein structure, makes the filament surface

(42) Zhou, Y.; Shimizu, K.; Cha, J. N.; Stucky, G. D.; Morse, D. E. *Angew. Chem., Int. Ed.* **1999**, *38*, 780.

(43) Niesen, T. P.; Bill, J.; Aldinger, F. *Chem. Mater.* **2001**, *13*, 1552.

inactive for bio-templating, further supporting the role of the protein surface in nucleation and/or growth.

Previous attempts, by Lee et al., at utilizing the $BaTiF_6$ single-source molecular precursor to make $BaTiO_3$ films by an elevated temperature liquid phase deposition method resulted in nonstoichiometric (ca. 1:11 Ba/Ti) and amorphous thin films.[25] Thus, it appears that the unique combination of the silicatein biocatalyst with $BaTiF_6$ leads to the formation of the high-temperature crystalline perovskite-like phase at low temperature, in which the 1:1 stoichiometry between barium and titanium is maintained. This is a significant result because it demonstrates that single-source molecular precursors can be used in conjunction with silicatein to grow nanocrystalline perovskite-like materials. Perovskite and perovskite-like materials have considerable technological value, which makes innovative low cost and/or low energy fabrication routes to kinetically controlled nanostructures extremely desirable.

Supporting Information Available: PCM hydrolysis calculations; FT-IR spectra of $BaTiF_6$, silicatein, and $BaTiOF_4$/silicatein; TGA traces. This material is available free of charge via the Internet at http://pubs.acs.org.

JA063107G